

# A review of the topographical causes of gloss variation and the effect on perceived print quality

Michael A. MacGregor<sup>1</sup>

## Abstract

It is well accepted that gloss variation deteriorates the print quality and there are various objective ways to measure this. Several studies now have shown that the coefficient of variation in the octave band passed *printed* gloss image has an excellent correlation with ratings by an expert panel using a magnitude estimation scaling method. The correlation improves when the gloss level is also taken into account beyond that of the COV. There is also evidence that the correlation would improve even more if the gloss spatial distribution could be better accounted for. We show that much (at least 80% and perhaps up to 90%) of the gloss distribution can be accounted for by the paper topography over a wide range of dimensions (scale). Recent work has supported the role that microroughness and multiple surface scattering play in the gloss distribution. This offers the promise of showing that even a greater amount of gloss variation can be explained by topography.

## Key Words

AFM, CLSM, gloss imaging, image analysis, terrain modeling, band passing, coated paper, multiple surface scattering, roughness, topography, print quality

## Introduction

This paper deals strictly with measurements of gloss variation from printed coated-paper surfaces (although some of the methods could also be used on uncoated surfaces or unprinted coated surfaces). This is mainly because our past work has shown the futility of predicting the printed gloss distribution from the unprinted white paper [1]. Printing can improve the gloss uniformity or it can make it worse, depending on numerous paper and printing variables.

---

<sup>1</sup> MacGregor Paper Consulting  
8 Pierce Court  
Appleton, WI  
<http://www.mac-paper.com>

Whether the viewer is aware or not, the printed paper surface is not seen under a single set of controlled conditions but under a multitude of illumination conditions. Not only does light arrive from various sources but also the viewer naturally moves the paper around during his viewing session, simultaneously changing both the incidence angle and the viewing angle.

Under these interactive dynamic viewing situations different paper surfaces react differently to these rather common (but scientifically challenging) viewing situations. Some paper appears good under certain conditions but then bad in others. Other paper seems to look good whatever the viewing/illumination conditions. What is the difference? What kind of paper can do this? Whether the paper (and its information content and the image that it was intended to portray) meets the expectations can be the difference between a fine advertising piece and one that's just commonplace.

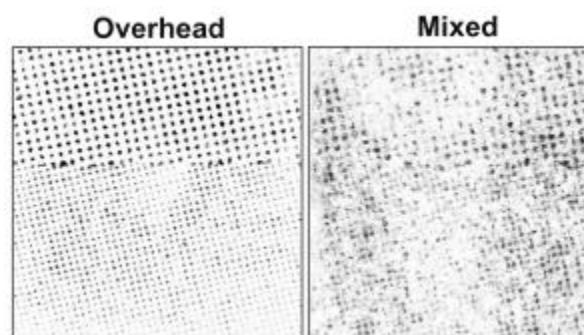


**Figure 1. Image of an LWC halftone print under two lighting conditions [2]. Note how in mixed illumination (overhead diffuse + gloss illumination) the specular reflection off the rough surface degrades the print quality, obscuring the original sharp dots (left).**

That the gloss distribution is an important determinant of final print quality is shown vividly in the registered image pair of Figure 1. Here it is seen in mixed illumination conditions (the way we often view prints) how the specular reflection from certain parts of the surface impedes information transfer. Not only does this specular reflection rob the print of its color saturation, many of the halftone dots are completely obscured. This large print information loss demonstrates well the importance of achieving uniform fine-scale gloss distribution.

This paper reviews gloss imaging methods and measurements and discusses some of the recent advances in measuring gloss distribution and its relationship to our perception of gloss uniformity. Also discussed is the

main source of gloss nonuniformity, the printed-paper topography at all dimensions down to the wavelength of light.

## Measuring gloss uniformity

### Gloss image acquisition

To acquire gloss images we use a CCD camera coupled to an image analyzer (Figure 2). This camera, with an acceptance angle of  $1.5^\circ$  and a  $20^\circ$  incidence angle, captures a 10 mm x 10 mm gloss image of the paper surface and is described in more detail elsewhere [2]. The gloss image image pixel size of about  $20\ \mu\text{m}$  is analogous to having  $\frac{1}{4}$ -million miniature gloss meters instantly measuring the specular reflection intensity from all parts of the printed paper surface. The resulting gloss image is comprised of many discrete reflection sources of various sizes (minimum pixel size of  $20\ \mu\text{m} \times 20\ \mu\text{m}$ ) that in turn form larger clusters of various sizes and shapes as seen in many of the images presented here. The relatively low  $20^\circ$  incidence angle is compatible with the way we view and judge prints for gloss uniformity because low incidence angle creates greater gloss contrast sensitivity, making it easier to see the gloss variation [2]<sup>2</sup>.

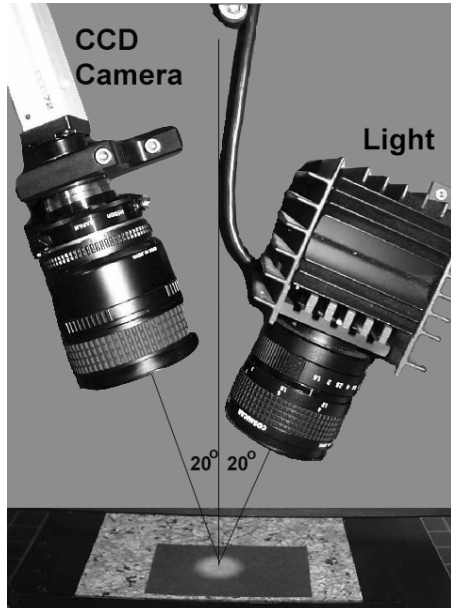


**Figure 2. STFI 20° Gloss imaging equipment [3] 10 mm x 10 mm field of view, 512 x 512 pixels, 20  $\mu\text{m}$  pixel size.**

<sup>2</sup> Viewing at high incidence angles makes every place appear glossy to the human visual system.

### Gloss image measurement

There are numerous ways to utilize the image analyzer for objectively measuring gloss images but we prefer the octave band passing method developed by Johansson [4]. We band pass the image into the sizes shown in Figure 3 and then calculate the coefficient of variation,  $V$ , for each of the bands (Table 1). We use the coefficient of variation because it normalizes the gloss variation to the gloss level and, in addition, previous work showed that the standard deviation had a low correlation with perceived gloss uniformity [1].

We think this behavior a fundamental result of the logarithmic response of the human visual system to light intensity. We also calculate the mid-range V35 octave bands (defined in Table 1) because the human visual system is most sensitive to these feature sizes at the viewing distances, approximately 25 cm, used in this work [5].

### Band passed gloss image

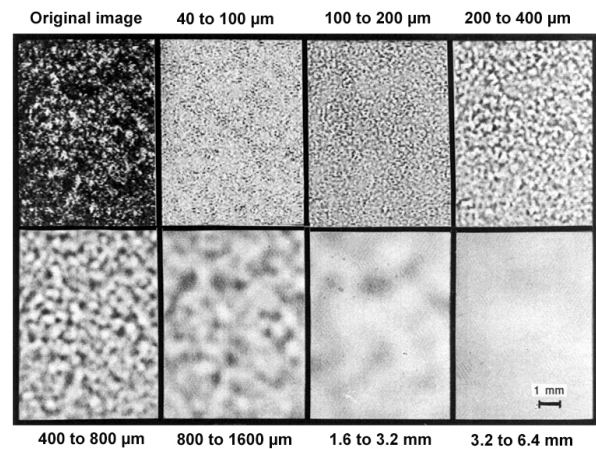


**Figure 3. Octave band passed images of original gloss image seen in the upper left [6]. The human visual system is most sensitive to feature sizes in the 200  $\mu\text{m}$  to 1600  $\mu\text{m}$  size range at normal viewing distances (ax. 25 cm).**

**Table 1. Octave band pass sizes and corresponding coefficients of variation for gloss image in Figure 3.**

Octave Band	Feature sizes	Coefficient of variation
Original image	all	48 %
1	20 to 50 $\mu\text{m}$	33 %
2	50 to 100 $\mu\text{m}$	23 %
3	100 to 200 $\mu\text{m}$	18 %
4	200 to 400 $\mu\text{m}$	14 %
5	400 to 800 $\mu\text{m}$	9.2 %
6	800 to 1600 $\mu\text{m}$	5.7 %
7	1600 to 3200 $\mu\text{m}$	3.2 %
3-5	200 to 1600 $\mu\text{m}$	17.7 %

Many other image processing methods not presented here can also be applied to extract useful information from the gloss image such as texture analysis, directional derivatives, slope, slope aspect, orientation filtering, autocorrelation, feature extraction, etc.[7].

## Relating gloss variation measurements to perception of gloss uniformity

### Gloss image coefficient of variation

Numerous gloss images of commercial LWC prints were acquired and octave band passing performed on these images. The print samples were also ranked by a panel of experts and these rankings then compared with the gloss variation in each octave band [1].

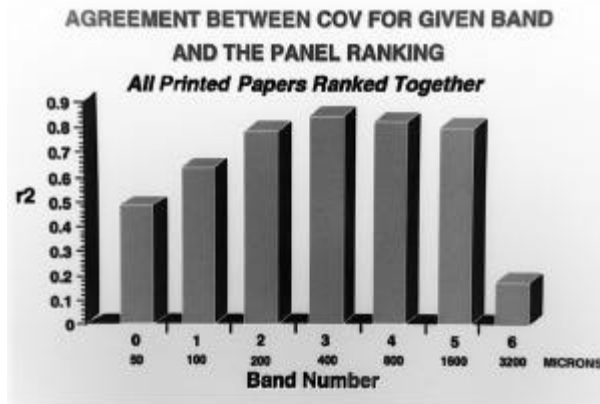


**Figure 4.** Perceived gloss uniformity vs. the measured gloss feature size [6]. Note the correlation peaks in the 400 to 800  $\mu\text{m}$  range, the area of highest spatial contrast sensitivity of the human visual system at the viewing distances used here ( 25 cm).

The results show (Figure 4) that the best correlation exists in the V35 size range (0.4 mm to 3.2 mm). This is consistent with the region of maximum spatial contrast sensitivity, 2-3 cycles/deg, for the human visual system [5]. Therefore, much of the work reported here the V35 data were used to compare with the print rankings and this gave quite a high correlation for such a simple image parameter (Figure 5).

A similar correlation coefficient between measured gloss variation and perceived gloss uniformity was found (Figure 6) in a more recent carefully conducted printing experiment using a large number of commercially manufactured and printed test samples[8].

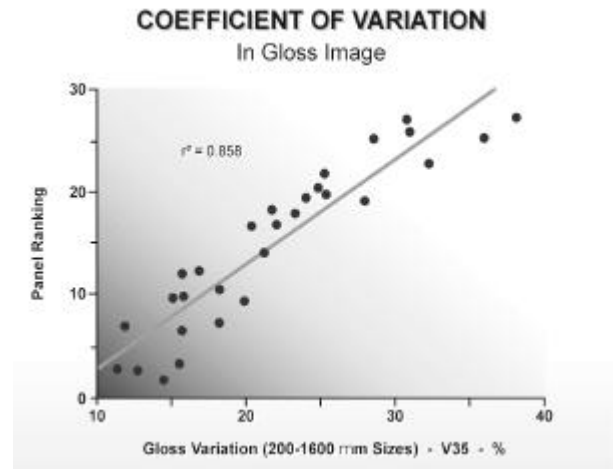


**Figure 5.** Measured mid-range gloss variation vs. perceived variation [6]. There is a surprisingly good correlation even with this simple single variable.

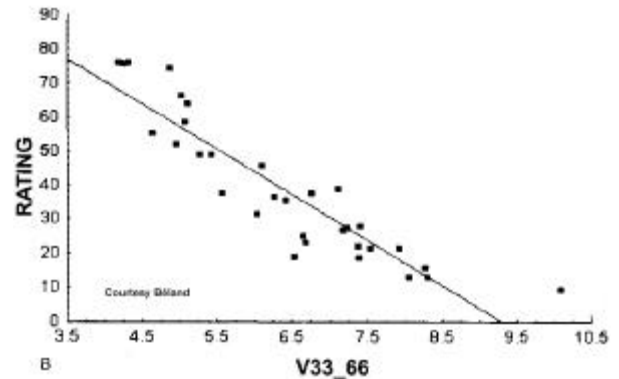


**Figure 6.** Panel rating (higher = better) vs. measured gloss variation using the magnitude estimation scaling method. Here the best spatial wavelength band was 3.3 to 6.6 mm, very likely due to the greater viewing distance used in this work, and the  $r^2 = 0.83$ . Data from Béland et al [8].

In this work the test samples were rated using magnitude estimation and multidimensional scaling methods [9],[10]. As opposed to the earlier average ranking method, these methods lead to the panel spacing their gloss uniformity ratings along a scale of preferences where a sample having twice the rating is preferred twice as much. The multidimensional scaling method also yields a threshold value below which the panel would find the print gloss variation unacceptable and thus is a more precise and accurate way to analyze the results.

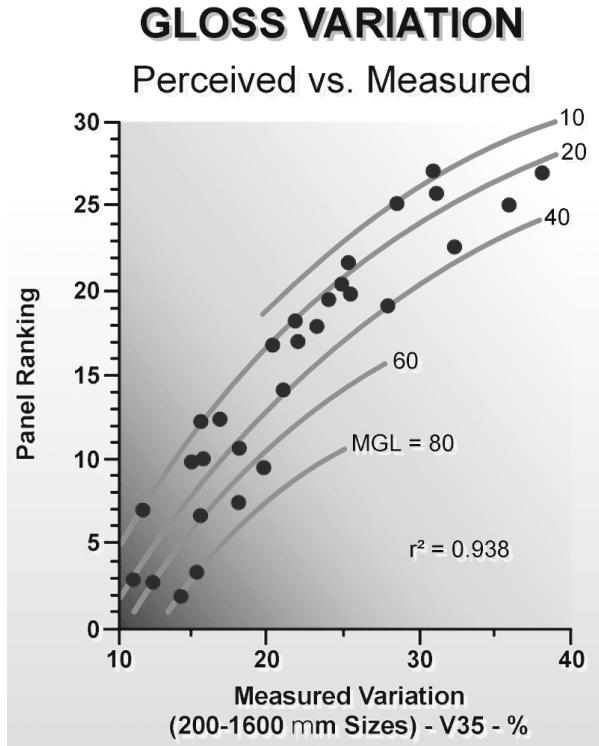


**Figure 7. Interrelationship between gloss variation and mean gloss level, MGL, as it affects the perception of gloss uniformity (1 = best) [1]. The smooth curves are derived from the regression equation with the dots being the actual data points for each gloss level. Note that in moving toward very high gloss levels the measured variation must necessarily reduce (it is physically impossible for highest gloss AND high COV to occur simultaneously).**

When the gloss measurements and ratings are subjected to a multiple nonlinear regression analysis with the gloss level as an additional variable, the correlation improves dramatically (Figure 7 and Figure 8). Though the gloss variation is obviously the strongest factor, the gloss level also plays a role. We think that viewers either accept higher gloss variation if the gloss level is higher or that it takes more gloss variation at higher gloss levels to be perceived—or both [1]. This still remains an area for further systematic investigation.

Both the works presented here, plus that of Shiratori et al [11], suggest that the methodology of acquiring gloss images, measuring them, and rating the corresponding prints agrees very well with our perceptions for a wide quality range of commercially manufactured coated and printed papers.

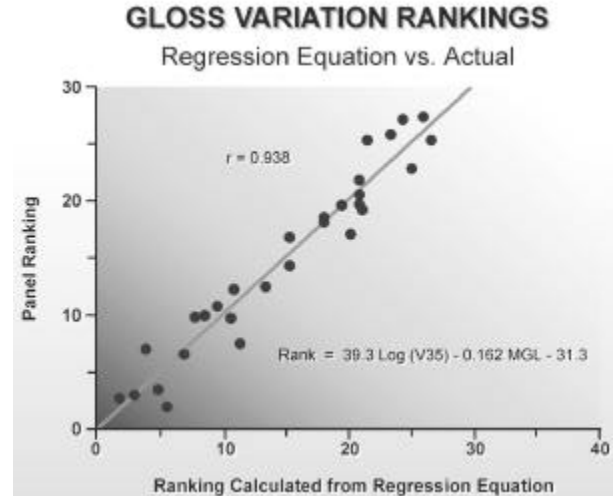


**Figure 8. Effect of including gloss level in the regression analysis [1]. Almost 95% of the variation in ratings is accounted for by the gloss variation and the gloss level.**

## Gloss spatial distribution

The octave band pass measurements of the gloss image reveals something about the size and intensity of high and low gloss areas but not about their spatial relationships (texture).

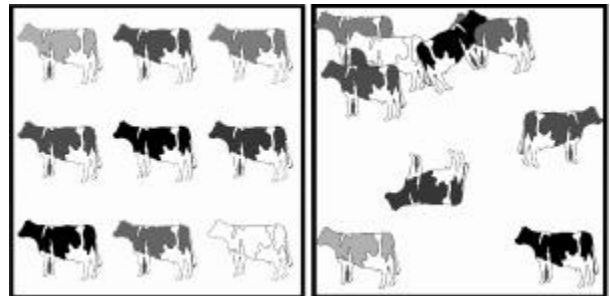


**Figure 9. Two images with identical coefficient of variation but different spatial distribution.**

The two images in Figure 9 illustrate this point. These images have nearly identical coefficient of variation, but obviously much different spatial distribution, and thus are perceived differently. Likewise, the three print samples in Figure 10 have identical gloss level and total gloss variation but were rated very differently by the expert panel.

Our experiments generally show that the human visual system has a preference for more uniformly spaced fine-scale gloss. The texture analysis methods referred

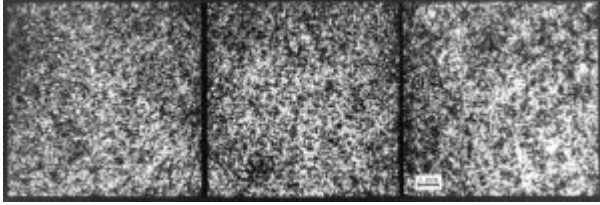


**Figure 10. The effect of gloss spatial distribution on perceived gloss uniformity for 3 LWC samples [1]. Surprisingly, the measured total variation is identical for all images but the actual print sample associated with the gloss image on the far left was perceived as most uniform. Our separate ratings of the actual print samples and their corresponding gloss images generally have excellent agreement. The white bar is about 1 mm long.**

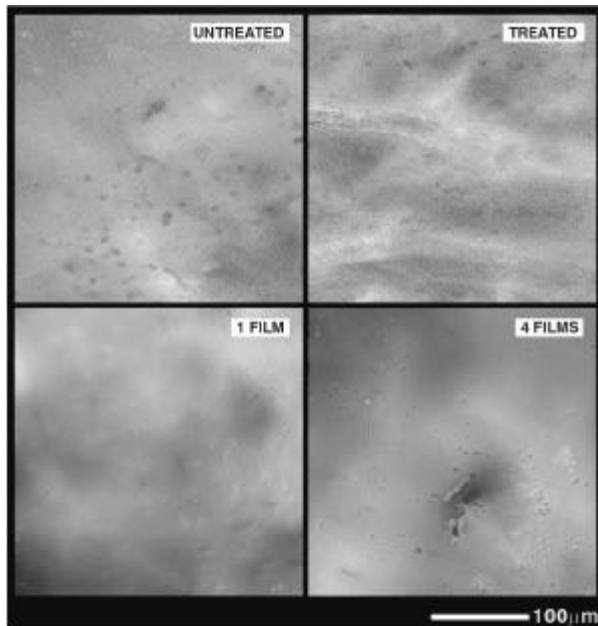


**Figure 11. CLSM of an LWC paper [12]. Original coated white paper (upper left) is printed with a thin film of water (upper right) and then roughens both on a macro scale (paper fibres) and a micro scale (produces a “graininess” in the coating). A single solid tone print film covers this micro roughness but 4 solid films actually increase the roughness in the form of larger pits (“blisters”) and tiny machine direction oriented pit trails. The surface also roughens on a macro scale due to the water emulsified in the ink.**

to earlier can perhaps provide another parameter for the data of Figure 7 and Figure 8 to achieve an even higher correlation.

## The topographical causes of gloss variation

Gloss *level* is a function of numerous variables but our work has shown that most of the gloss *variation* on a coated printed surface arises directly or indirectly from topography variations at various dimensional scales. Surprisingly, this holds true for even the flattest highest-quality surfaces. A close study of the “grainy” features in Figure 11 shows that the dried ink film covers very small surface features ( $< 1 \mu\text{m}$  or less) with a highly reflective layer but nonetheless introduces topographical variations of its own.

The 100% ink film coverage results from the flattening that even a very rough coated paper surface such as LWC undergoes inside the printing press nip. This gives a compressed surface volume far less than the ink film volume available on the blanket (Figure 12), thus forcing the ink to flow into all places.

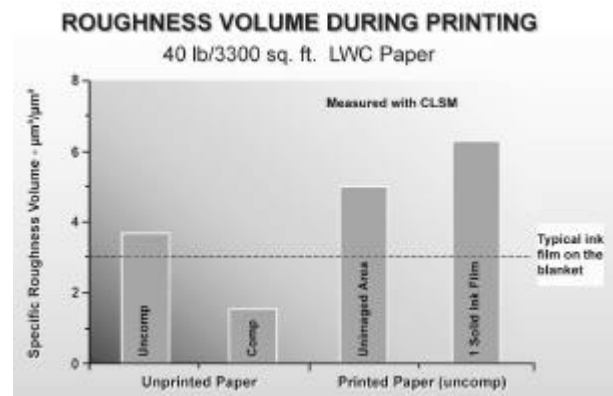


**Figure 12. Surface roughness volume of LWC paper during printing [1]. The paper flattens in the printing nip and the roughness volume is far less than the volume available on the blanket. There is essentially 100% ink film coverage for a solid tone.**

So, except for the lighter halftones, the ink *covers* the entire surface with a reflective film but for rough papers like LWC it cannot *fill* the roughness volume with ink (Figure 13), leaving a rough but highly reflective surface.

This is a recipe for large gloss variations. Further, certain papers like LWC exhibit water-induced roughening during the printing process [12]. Our confocal microscopy shows the paper often is rougher in the imaged areas than the unimaged areas (Figure 12 and Figure 14) and we think this is evidence of more water being emulsified within the ink than applied from the fountain solution on the blanket.

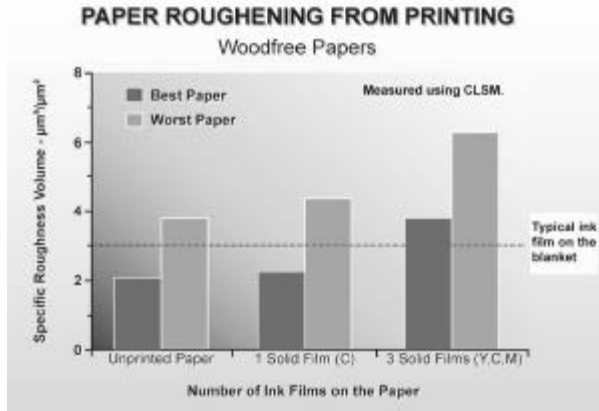


**Figure 13. Surface roughness volume for the roughest and smoothest coated woodfree publication papers [1]. While the ink film can fill the smooth paper surface to a level condition, there is insufficient volume to fill the rough paper surface. All papers generally become rougher with more solid ink films.**

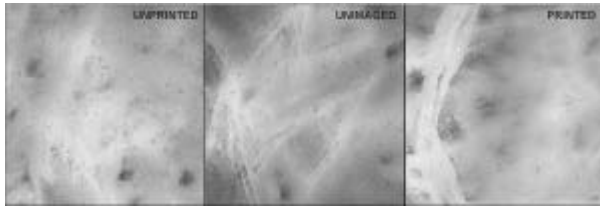


**Figure 14. Water-induced roughening of a solid tone LWC paper [13]. The paper is rougher on the macro scale due to the water from the fountain solution in the unimaged area (center) and from that emulsified in the ink in the imaged area (right). This is strong evidence that more water is emulsified in the ink than transferred to the unimaged area and the resulting water-induced roughening makes the printed area rougher. The water amplifies the coating “graininess” seen in the unprinted (far left) and unimaged (center) areas of the paper but the ink can cover it (far right).**

Lastly, the surface roughness results in a thinner ink film (lower density) on the high areas as shown by the light areas in Figure 15 and also reported by others [14]. The reflective rough surface combines with this ink density variation to create a “gray” look and reduce the color saturation. This greatly inhibits the information transfer of the printed image, thus degrading the print quality.

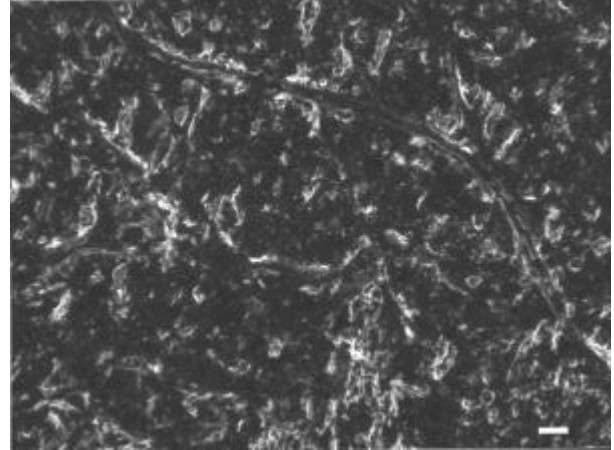


**Figure 15. Solid tone ink distribution on a rough LWC paper seen in diffuse overhead illumination [13]. The high places have much lower ink density (ink film thickness) but are still covered with a reflective film that gives reflections in many directions. These, along with the ink density variation, impart a grayish cast to the print and rob it of its color saturation.**

## Direct experimental evidence of the gloss/topography relationship

### Gloss/Terrain-Modeling of an LWC printed paper

LWC paper, though coated and supercalendered, possesses one of the lowest-quality coated paper surfaces. Because of its numerous rough and sloped areas, it was expected to produce the best relationship between gloss and topography. However, we have found that the methods also work well even for very smooth high-quality surfaces.

The gloss image is obtained with the STFI 20° gloss imaging equipment while the topography map is *independently* obtained at the same place in the paper by a confocal laser scanning microscope (CLSM). We used an LWC paper printed solid black, enclosing several high gloss features within scalpel marks. The registered image pair is shown in Figure 16.

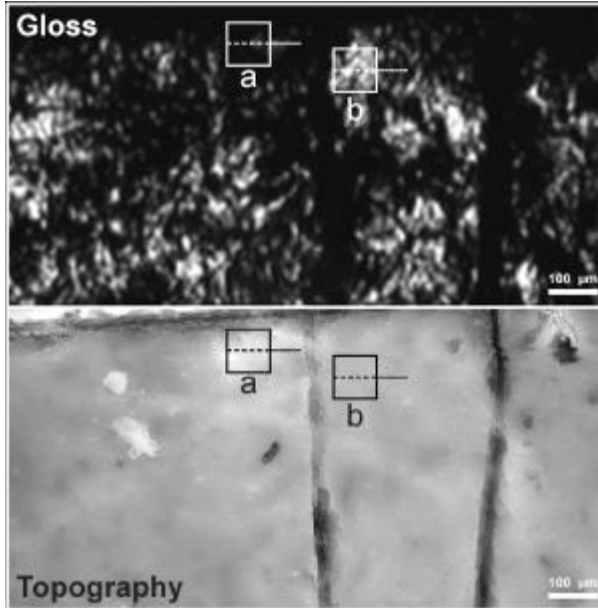


**Figure 16. Topo/Gloss registered image pair for an LWC printed paper [1]. In the topo image, higher elevations are brighter. Note the deep vertical and horizontal dark marks that were used to bound several bright areas in the gloss image. These marks were made with a scalpel using the gloss imaging equipment to locate the bright areas (zero incidence angle illumination). Several fibres are seen lying in the coating in the topo image. They cause dark areas in the gloss image due to the slope they give the surface.**

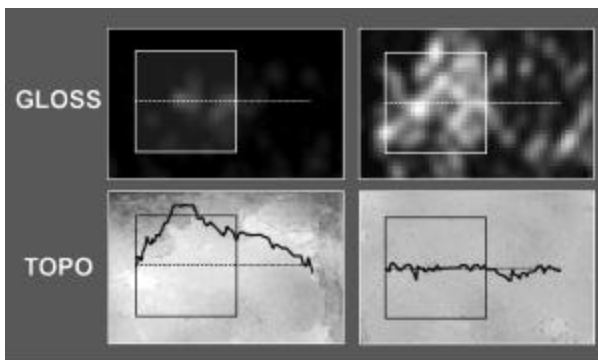


**Figure 17. Height profiles of the two features extracted from the topo and gloss images [1].**

Visual inspection shows good general agreement between the two images. For example, the scalpel marks and the surface debris in the topo image all agree with low gloss areas in the gloss image. Likewise, the effect of several fibres lying within the coating is seen in the gloss image. Two features marked *a* and *b* are shown in greater detail in Figure 17. The low-gloss feature *a* agrees with a mountainous feature and the

high-gloss feature *b* agrees with the flat place. Note the barely discernible reflection still being produced by the tiny ( $\approx 25 \mu\text{m}$ ) flat top of the mountainous feature. Note also that even the very flat high-gloss area still has significant gloss variation on the micro scale.

Many such individual surveys were performed on this image-pair and this encouraged the development of the facet angle mapping method described elsewhere [15] and ultimately the utilization of geographical information systems (GIS) terrain modeling techniques for characterizing surfaces and 2-dimensional data sets in general [7].

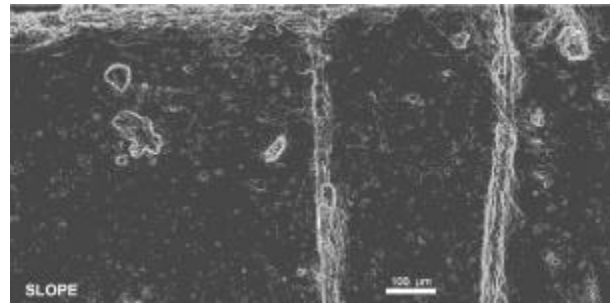


**Figure 18. Slope map (UW—Madison, WI image). Derived from the topo map in Figure 16 using the ERDAS GIS program [7]. Steep slopes are lighter.**

Figure 18 shows a slope map derived from the original topo map (Figure 16). Feature *a* with its small flat top is easily seen in the slope image as are the scalpel marks. Several horizontal fibres are barely discernible in the slope image (at high magnification) but become much more evident in the slope aspect image (Figure 19) because their gently sloping sides face along a common Northerly/Southerly direction.

Other dimpled surface textures, not seen in the topo or slope maps, are nicely brought out in the slope aspect image. These likely agree with the thick very gently sloping coating areas discussed in the “orange peel” work [16]. Regions containing a fine-scale uniform mixture of all slope directions are the flat places that generally agree with the bright areas in the gloss image. Lastly, the slope aspect image shows both large and small-scale feature directionality. The large-scale CD-oriented features could be related to the coating and/or calendering processes. This possibility likely could not have been discovered without the new information provided by the slope aspect map.<sup>3</sup>

<sup>3</sup> Compared to the gray level image shown here, all these features are seen better in the original 8-color slope aspect image.

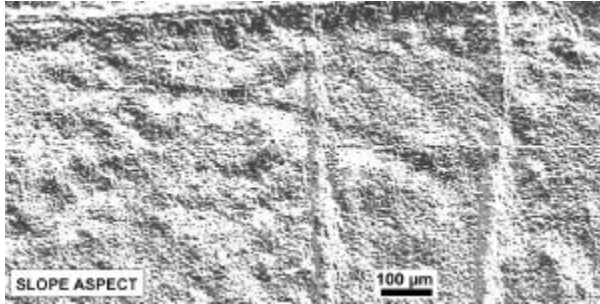


**Figure 19.** Slope aspect map (UW—Madison, WI image). Derived from the topo map in Figure 16 using the ERDAS GIS program [7]. Original is an 8-color image whose colors divide into 8 major compass settings.

In the gloss imaging equipment it requires less than  $1^\circ$  tilt for the reflected light from a surface to drop by 50% and only  $2^\circ$  for it to drop to essentially zero, Figure 25 [1]. The slope map was therefore thresholded at  $1.5^\circ$  and the gloss image at a gray level of 40 to give the binary image pair shown in Figure 20. Here the bright places in the gloss image and the “flat” places in the facet angle map are colored white and have about equal area in each image, supporting the threshold choice. An auto correlation between the two images found about 80% spatial agreement ( 60% low-gloss places located in the tilted areas and 20% high-gloss places located in the “flat” places). The remainder (20%) is not accounted for by the gloss-topography relationship.

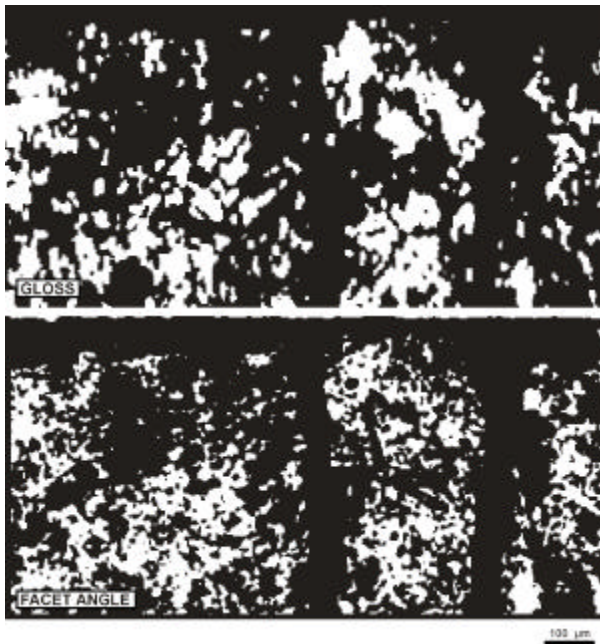


**Figure 20.** Gloss/Facet Angle registered 2-color image pair [1]. Places above a gray level of 40 are called “high-gloss” and are colored white in the gloss image (25%). Places with less than  $1.5^\circ$  slope

are called “flat” and are also colored white (26%). The visual agreement is remarkable considering that the two images are derived from completely independent data. Pixel size for the gloss image is about  $20\ \mu\text{m}$  and that for the facet angle image about  $5\ \mu\text{m}$ .

## Gloss/Topography failure analysis

The 20% spatial failure of the gloss/topography relationship shown in the previous section was about evenly split between tilted/glossy and flat/low-gloss places. Some of these failures could be due to slight misregistration between the image pair and also to the different pixel sizes used in the two images. Some of the failure also has a possible physical explanation in either local microroughness or light reflecting several times before it leaves the surface (multiple surface scattering).

### Flat/Low-Gloss failure (local microroughness survey)

None of the measurements reported in the previous section addressed the micro scale roughness (near  $1\ \mu\text{m}$  and below). A “flat” area in the slope image where all the  $5\ \mu\text{m}$  facets making up that area had less than  $1.5^\circ$  slope could appear dark in the gloss image if that area was also rough on the micro scale (optically rough).

Recent work combining the gloss imaging equipment with the CLSM and atomic force microscopy (AFM) was performed in a first attempt to test this idea on two matte-coated 400% black printed papers [17]. The best and the worst ranked samples were chosen for study and, from these, high and low gloss areas identified (Figure 21). The AFM was used to image and measure different areas within each CLSM image for local roughness. These high and low gloss areas had been located in the corresponding registered gloss image so that a comparison between the gloss, CLSM, and AFM images could be made.<sup>4</sup>

Places in the low-gloss regions of the CLSM were found in the AFM that belonged to the tilted/smooth category. For example, on one of the low-gloss areas of the best sample, a slope of about  $4.4^\circ$  and an  $R_q$  of

<sup>4</sup> The AFM survey was conducted within the CLSM field of view that itself was located in a high or low gloss region of the gloss image.

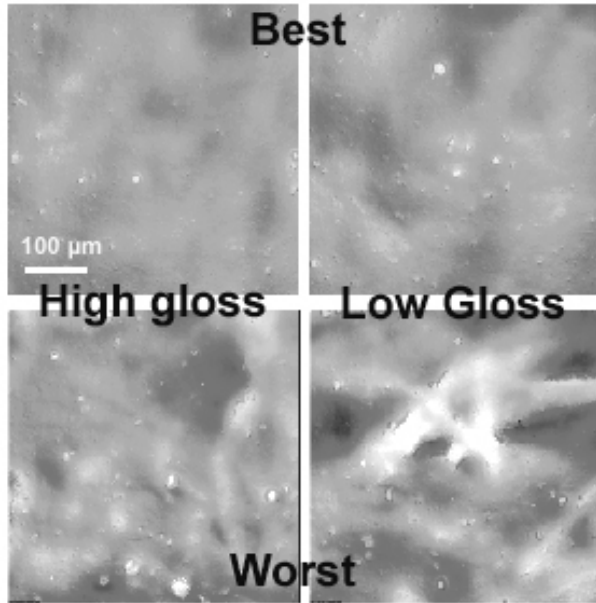


**Figure 21.** CLSM topo maps of the Best (upper pair) and Worst (lower pair) samples printed 400% black [17]. 500  $\mu\text{m}$  x 500  $\mu\text{m}$ . A high-gloss (left side) and a low-gloss area (based on the registered gloss image) are shown for both samples. The AFM was used to measure the roughness of local areas (25  $\mu\text{m}$  x 25  $\mu\text{m}$ ) in these CLSM images.

0.61  $\mu\text{m}$  were measured. After mathematically flattening (untilting) the topographical data for this local area and then recalculating the roughness, the slope was removed and the roughness,  $R_q$ , dropped to 0.14  $\mu\text{m}$ . Obviously, this was a locally smooth area that was tilted too far away from the specular reflection plane to appear glossy. The tilt of this area also made the original calculated local roughness much higher than it actually was. The gloss-topography relationship would have been directly proven were it possible to accurately identify this *exact* AFM area in the gloss imaging equipment and then untilt it by  $4.4^\circ$  to confirm that it indeed turned glossy.

Other low-gloss areas were identified that in the AFM image turned out to be flat but rough. For example, on one of the low-gloss areas of the worst sample, an  $R_q = 0.54 \mu\text{m}$  was obtained before mathematically flattening the topo image but only dropped to  $R_q = 0.49 \mu\text{m}$  after flattening. This low-gloss area was well within our definition of “flat” (less than  $1.5^\circ$ ) but it was optically rough enough to scatter the light instead of specularly reflecting it back into the gloss-imaging camera as a bright spot.

Because the AFM field of view and vertical range is so small, this method cannot be used to determine exactly how much of the surface is locally smooth or rough—

only to prove that these areas do exist and that they invariably agree with the local gloss level. This work indicates that if it were possible to sense local microroughness at sufficient resolution *and* field of view the results would presumably be compatible with the 10% flat/low-gloss failure under the gloss image acquisition conditions used here (Figure 20).

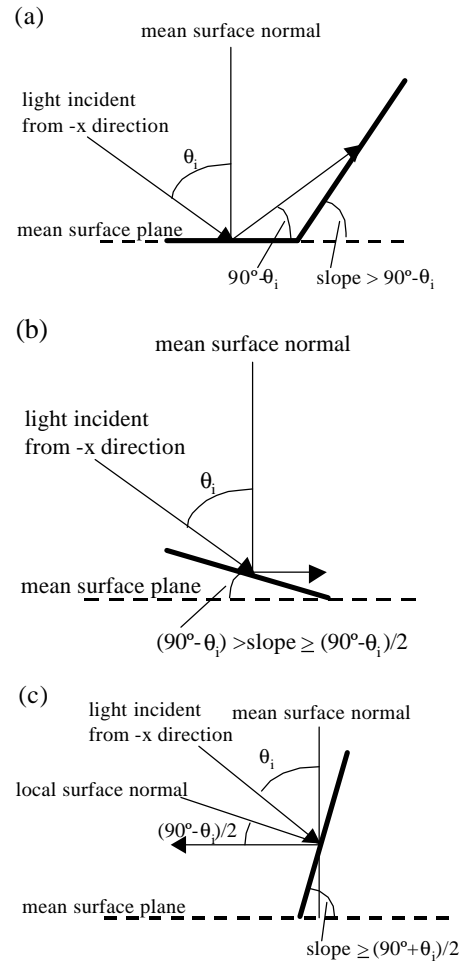


**Figure 22.** General conditions for multiple scattering (a) from a flat area having a highly sloped neighbor facing the incident direction; (b) from areas facing away from the incident direction but having a large enough slope to reflect the light towards the surface; and (c) from areas facing the incident direction with large enough slope. All these conditions assume that the local microroughness of the facet is less than 1.5  $\mu\text{m}$ . [18] For the  $20^\circ$  gloss imaging work reported here the slope angle values for the three conditions would be (a) less than  $70^\circ$ , (b) between  $35^\circ$  and  $70^\circ$ , and (c)  $55^\circ$  and greater.

## Tilted/High-gloss failure (multiple light scattering)

There is another gloss-topo failure for this particular LWC paper example that still has not been rationalized—tilted/glossy areas.

Recently, Béland [18] modeled the theoretical possibility of light reflecting one or more times before leaving the paper surface (multiple light scattering). This can occur when certain surface geometry conditions are met (Figure 22). For smooth paper surfaces, multiple surface scattering becomes significant only at large incidence angles (Figure 23a). At the low incidence angle ( $20^\circ$ ) used in the work reported here there is little chance of meeting the geometry requirement for multiple scattering off smooth surfaces because even the most tilted smooth areas of a low-quality paper like LWC have slopes that are quite low (typically much less than  $10^\circ$ ).

The likelihood for multiple scattering is much greater off rough tilted facets (Figure 23b). Here, the facet micro topography creates local surfaces that direct some light toward neighboring facets. If these neighbors are tilted correctly, this light is in turn reflected off the surface at the mean plane specular reflection angle. This has the effect of making the original area appear dark and some areas appear glossy that would not otherwise have.

The multiple scattering model (which utilizes actual topographical data as input) gives results (Figure 23) that are compatible with the tilted/glossy failure category (about 10% in the example given here). For the  $20^\circ$  incidence angle used here, this model applies mainly to very small areas, not necessarily explaining the larger-size ( $100\ \mu\text{m}$  and larger) tilted/glossy failures encountered. The model calculates the proportion of the surface that can potentially cause multiple light scattering and also can give the spatial distribution where multiple light scattering occurs (image not shown here). However, in this first investigation it unfortunately was not possible to test the model by directly comparing this spatial distribution to the corresponding gloss image, an interesting possibility for future investigation.

This model provides much insight into the behavior of light on paper surfaces. And, it provides promising evidence that a rough paper surface can theoretically give multiple light scattering in amounts consistent with the earlier results of 10% for the tilted/high-gloss failure mode.

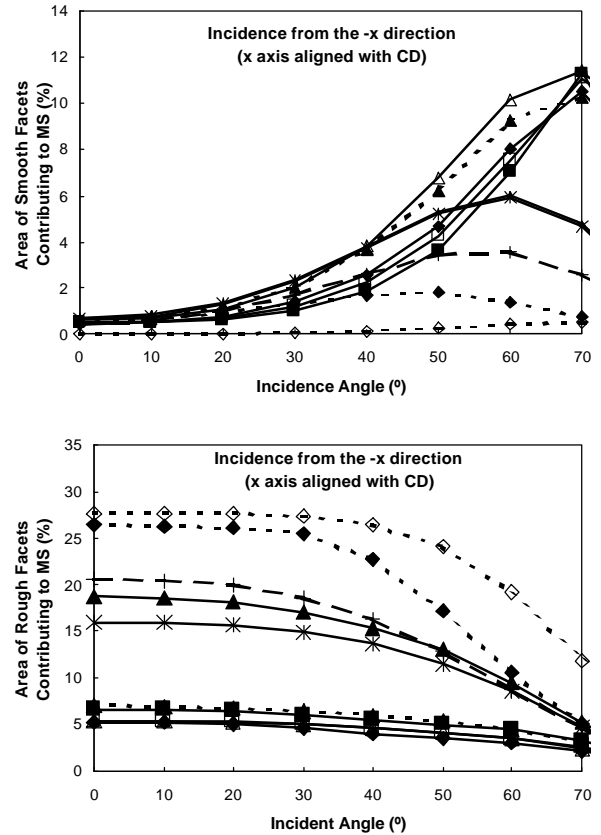


**Figure 23.** Area of the surface contributing to multiple surface scattering as a function of incidence angle and facet microroughness for ten printed samples [18]. Each curve represents an average of either two or three measured areas. The incidence plane was (a) parallel to the cross-machine direction of the paper with the light incident from the -x direction, and only *smooth* facets are taken into account and (b) the same but only *micro rough* facets are taken into account.

## Incremental tilt angle imaging to locate tilted/flat and flat/rough places—a proposed method

Our original investigations [19] revealed that paper surfaces react very differently to tilting in the gloss imaging equipment, shown dramatically in Figure 24. This suggests additional possibilities for utilizing the equipment to better characterize the printed surface.

By mounting the sample on a rotate-able cylindrical surface Lindstrand [20] developed an elegant image analysis method that measured the reflection intensity of each pixel in the gloss image as a function of tilt

angle from the specular mean plane. He then used this information to derive a facet angle map.

Taking that approach further, it is proposed here to use the STFI gloss imaging system to perform incremental tilt angle gloss imaging *in two orthogonal planes*, recording the 2-dimensional reflection behavior of each pixel. This could yield new images from which the “dynamic” gloss behavior of the surface might be quantified.

Using light as a tool to probe the surface, the optically rough and optically smooth places could be indirectly derived over a large image area and good resolution by keeping track of the reflection behavior of every pixel (e.g., Figure 25)—a kind of a 2D directrix map for the entire surface. The proposed method utilizes the gloss imaging equipment, modified to acquire gloss images at small tilt angle increments in each of both planes (X and Y directions) to either side of the specular mean plane. In general, all places that remain dark through a wide range of (x,y) tilt angles are assumed optically rough. All dark places at the mean specular plane that eventually turned glossy at some (x,y) tilt angle are assumed optically smooth (but tilted).

Incremental tilt angle gloss imaging could also give other important information—an idea of the “dynamic” gloss behavior for a printed surface. Assimilating the surface quality of prints by moving them around in various lighting is, after all, the way we view and judge them.

Extremely flat and smooth surfaces should be very sensitive to tilt angle, *everywhere quickly* losing specular reflection intensity with small tilt angles (Figure 24). They would be characterized as being dynamically stable because the gloss distribution would change very little between its “on” and “off” conditions.

Extremely smooth but undulating surfaces (hammered surface look) might be classified “unstable” because the large-scale gloss distribution would change rapidly with small tilts.

Rougher undulating surfaces would also be sensitive to tilt angle because there are so many facets lying at different angles from which light is reflected or multiply-scattered over a wide range (Figure 1). This would cause the gloss distribution to shift, with small areas alternately becoming glossy or dark as the sample was tilted. The range over which this occurred and the amount of shifting could characterize the “gloss instability” of the surface.

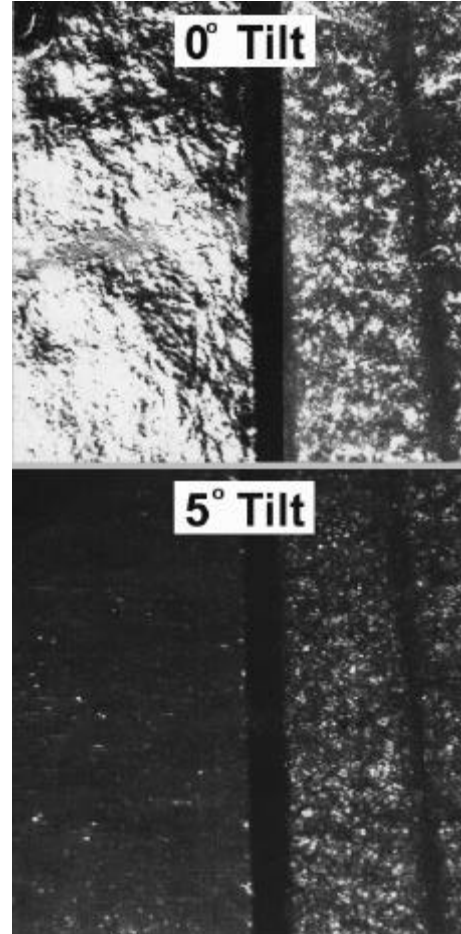


**Figure 24.** Effect of single-plane tilting of unprinted samples in the gloss imaging equipment [19]. After tilting, the cast-coated sample (left) has virtually no places that reflect light into the camera while the rough LWC (right) still has many places even at this high tilt angle. Though held down with double-sided tape, the cast-coated sample was not exactly flat, showing extreme sensitivity to local tilt angle variations (upper left image). During tilting the cast-coated gloss dropped immediately to nothing after only several degrees tilt. Registered images are 10 mm on a side.

Lastly, a paper with a combination of optically smooth and rough patches (e.g., the “orange peel” patterns [21]) would probably behave the worst because these medium-scale changing gloss patterns would be especially noticeable to the viewer.

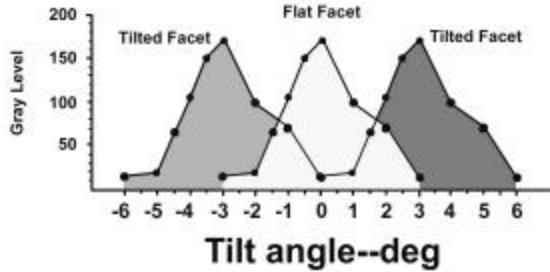


Figure 25. Reflection intensity behavior of model facets during gloss image tilting (based on actual measurements [1]). The reflection intensity peaks indicate that the two facets either side of the flat facet are tilted by 3°. When the sample is flat (0° tilt), the smooth/flat facet (middle) reflects maximum intensity while the smooth/tilted facets (either side) reflect little. If the sample were tilted, the flat facet intensity would greatly lower and the tilted facet greatly increase, peaking out at 3° and then rapidly dropping with further tilting. The tilting must be done in at least 2 orthogonal planes to determine both the facet slope and its aspect (direction).

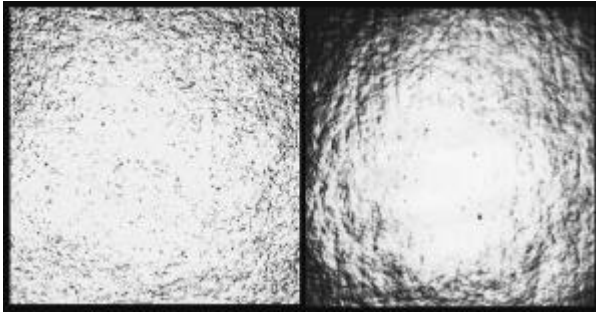


Figure 26. Gloss images of an unprinted No. 1 Coated Publication paper (left) and a cast-coated paper (right) [19]. 10 mm x10 mm field of view. Note the sheen compared to the LWC papers of Figure 10. Even the cast-coated paper has a certain roughness but also a much more contiguous high-gloss than any other paper. Emphasizing the sensitivity this particular surface has to the gloss illumination, the straight vertical marks in the coating replicate grinding marks in the drying cylinder! The very high-gloss surface of the cast-coated produces an extremely sharp gloss fall-off as seen by the circle of light that represents the illumination light source in the gloss imaging equipment. The very high-quality publication paper also shows a gloss falloff at the corners but not nearly as sharp the cast-coated exhibits. A glass plate (used in aiming the light source) would exhibit a centered white circle.

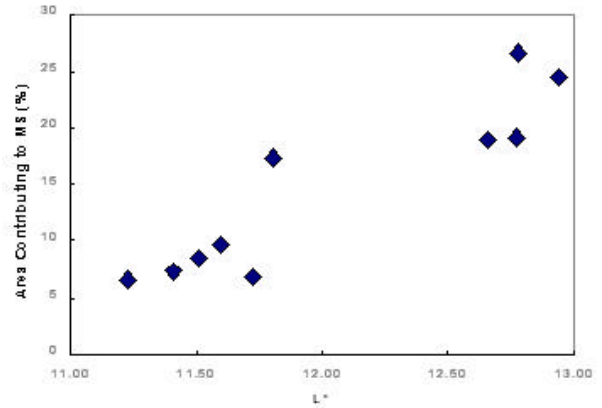


Figure 27. The  $L^*$  value represents the blackness of the print, 0 being black and 100 being white. The  $L^*$  value of the black, printed samples is plotted here against the calculated area contributing to multiple scattering using an incidence angle of 40°. The correlation coefficient is  $r^2=0.85$ . From Béland [18].

### Final comments—the gloss “look”

The “look” of a printed surface is an issue not touched on by any work reported here. Yet, some panel members were strongly influenced by, for example, a “gray look” when making their ratings. Other panelists could have been influenced by this “gray look” without realizing it. The gray appearance is believed caused by light specularly reflecting off microscopically tiny facets (e.g., edges of fibers lying in the coating, cracks in the coating, etc.), especially in a rougher surface. This “gray look” hinders our ability to sense a “depth” to the printed surface—like tiny breeze-blown ruffles or even a dust film on an otherwise crystal-clear pond surface. The ideal printed surface in most cases is one that does not “get in the way” of the printed information but indeed enhances it.

Just as for other subjective names given to the appearance of glossy papers (e.g., “icy,” “silky,” “hazy,” “hammered”), the measuring methods discussed here do not address properties that we still think are important and may originate at the light wavelength dimension. Somehow, methods to objectively measure this quantity must be found because it is such an important attribute of our judgment of printed surface quality—especially for high-quality printing papers.

One such attempt was recently made by Béland [18] where the calculated multiple scattering area of prints (Figure 23) was compared to the  $L^*$  value, a colorimetric measure of the blackness level (Figure 27). The good correlation achieved gives encouragement to

further investigate the “grayness” of prints, including in the investigations the magnitude estimation and multidimensional scaling methods mentioned earlier.

In a concluding remark, the dichotomy in all this is that, although our gloss images had a 20  $\mu\text{m}$  pixel size (orders larger than the wavelength of light), these images still managed to convey to us a sense of “silky” appearance for the best papers (e.g., Figure 26). There is something about the human visual system that allows us to perceive this appearance even with pixels this large, proving that, as always, gloss is a complex psychophysical phenomenon.

## Conclusions

Gloss variation in prints is bad because the noise it introduces reduces information transfer and is annoying to the viewer. As important in the commercial world, the aesthetic degradation inevitably attaches by association a lesser quality to the information or actual subjects being depicted in the print.

The image analysis methods discussed here provide fast and simple objective measurements that agree well with the human visual system. Still, these methods could be improved to account better for the spatial distribution (texture) effect on the human visual system.

Almost all the important gloss variation in printed coated papers is found to either originate with or is associated with topographical features over a wide range of dimensions down to the wavelength of light. In this particular work, up to 90% of the gloss variation was possibly accounted for by topography. Future work could bring this agreement even higher.

Lastly, a proposed new method for characterizing the “dynamic” gloss behavior of the printed surface is mentioned. This is based on an image analysis procedure called “incremental tilt gloss imaging” and utilizes light as a tool for quickly finding optically rough or optically smooth but tilted places. From this, microroughness, slope, and slope aspect mapping is possible over a large field of view and at good resolution—something we cannot do presently.

## Acknowledgements

In the scientific world, nothing happens in a vacuum. I therefore express sincere appreciation to my fine colleagues in Sweden, Marie-Claude Béland (ACREO), Per-Åke Johansson (STFI) and Siv Lindberg (STFI Perception Laboratory) for the collaborations we’ve had over many years in this very interesting and exciting area. I also especially thank Marie-Claude Béland for permitting me to include some of her latest work here, for various image analysis measurements, and also for her discussions and critique of this manuscript.

Presented at the Hansol Symposium 2000, Seoul, Korea, Dec 1, 2000

Note: To properly observe the details of certain images in this paper, it is important to view them at much higher magnification. For this purpose, this paper can be made available in a high-resolution electronic format for on-screen viewing or printing. Please contact the author [mike.macgregor@mac-paper.com](mailto:mike.macgregor@mac-paper.com) for details.

## Literature cited

1. MacGregor, M.A., P.-Å., Johansson, and M.C. Béland. *Measurement of small-scale gloss variation in printed paper: topography explains much of the variation for one paper*, in *TAPPI/CPPI International Printing and Graphic Arts Conference*. 1994. Halifax, Nova Scotia, Canada: Canadian Pulp & Paper Association.
2. MacGregor, M.A. and P.-Å., Johansson, *Submillimeter gloss variations in coated paper; Part I, the gloss imaging equipment and analytical techniques*. *Tappi Journal*, 1990. **73**(12): p. 161-168.
3. Béland, M.-C. and J.M. Bennett, "Using CLSM and AFM to assess the gloss uniformity of printed paper", in *Proceedings of the Microscopy as a Tool in Pulp and Paper Research and Development Symposium*. 1999. Stockholm, Sweden.
4. Johansson, P.-Å., *Evaluation of grey tone evenness using band pass filtering*, in *3rd Scandinavian conference on image analysis*. 1983. Lund, Sweden.
5. Campbell, F.W. and Maffei, L., *Contrast and spatial frequency*. *Scientific American*, 1974. **231**(5): p. 106.
6. MacGregor, M.A. and P.-Å. Johansson, *Gloss uniformity in coated paper*, in *Tappi Coating Conference*. 1991: TAPPI Press.

7. Andersson, M., *Application of image processing techniques to paper analysis*, Master's Thesis in Dept. of Electrical Engineering. 1998, Linköping Tekniska Högskola: Linköping, Sweden. p. 44.
8. Béland, M.-C., S. Lindberg, and P.-Å. Johansson, *Optical Measurement and Perception of Gloss Quality of Printed Matte-Coated Paper*. Journal of Pulp & Paper Science, 2000. **26**(3): p. 120-123.
9. Stevens, S.S., *Psychophysics: Introduction to its Perceptual, Neural, and Social Prospects*. 1975, New York: Wiley.
10. Donderi, D.C., *Information measurement of distinctiveness and similarity*. Perception and psychophysics, 1988. **44**(6): p. 576 to 584.
11. Shiratori, N., H. Ishimura, and N. Yoshidomi, *Study on quantitative evaluation of submillimeter gloss variations in coated papers*, in *TAPPI Advanced Coating Fundamentals Symposium*. 1993. Minneapolis, MN USA: Tappi Press.
12. MacGregor, M.A., *Measuring water-induced roughening of LWC paper and its effect on printed gloss*, in *Process and Product Quality Conference*. 1996. Cincinnati, OH: TAPPI Press.
13. MacGregor, M.A., *A procedure to measure print roughening propensity in LWC paper and predict its effect on the final printed gloss*, Internal Technical Report, 1995, Voith, Inc.: Appleton, WI.
14. Gregersen, Ø.W., Johnsen, P.O. , and and T. Helle, *Small-Scale Topographical Variations of Newprint Surfaces and their Effects on Printing Ink Transfer Distribution*. JPPS, 1995. **21**(8): p. 285.
15. Béland, M.-C. and C. Barratte, *Facet angle mapping of paper topography*. Internal Scientific Report, 1995, Pulp and Paper Research Institute of Canada: Pointe Claire, Canada. p. 1-16.
16. MacGregor, M.A. and P.-Å. Johansson, *Image analysis techniques for studying "orange peel" gloss effects in a LWC paper*, in *Tappi Coating Conference 1990*: TAPPI Press.
17. Béland, M.-C. and J.M. Bennett, *Effect of local microroughness on the gloss uniformity of printed paper surfaces*. Applied Optics, 2000. **39**(16): p. 2719-2726.
18. Béland, M.-C., *Multiple Surface Scattering of Light Calculated from the Topography of Printed Paper Surfaces*, PhD Thesis in Dept of Physics, Royal Institute of Technology: Stockholm, to be published.
19. MacGregor, M.A., *Exploratory investigations of high-incidence-angle gloss imaging*, Internal Scientific Report, 1989, KTH: Stockholm.
20. Lindstrand, M., *A conceptual approach to describe gloss variation in printing paper*, Master's Thesis in Dept. of Electrical Engineering, Linköping Master's Thesis, LiTH-ISY-EX-1624, Linköping University, Sweden, (1996).
21. MacGregor, M.A. and P.-Å. Johansson, *Submillimeter gloss variations in coated paper; Part 2, Studying "orange peel" gloss effects in a lightweight coated paper*. Tappi Journal, 1991. **74**(1): p. 187-194.